chemosensors

MDPI

Article

Enhanced Sensitivity and Homogeneity of SERS Signals on Plasmonic Substrate When Coupled to Paper Spray Ionization–Mass Spectrometry

Adewale A. Adehinmoye, Ebenezer H. Bondzie, Jeremy D. Driskell *, Christopher C. Mulligan * and Jun-Hyun Kim *

Department of Chemistry, Illinois State University, Normal, IL 61790, USA; adehinaa@mail.uc.edu (A.A.A.); ehbondz@ilstu.edu (E.H.B.)

* Correspondence: jdriske@ilstu.edu (J.D.D.); cmullig@ilstu.edu (C.C.M.); jkim5@ilstu.edu (J.-H.K.)

Abstract: This work reports on the development of an analyte sampling strategy on a plasmonic substrate to amplify the detection capability of a dual analytical system, paper spray ionization–mass spectrometry (PSI-MS) and surface-enhanced Raman spectroscopy (SERS). While simply applying only an analyte solution to the plasmonic paper results in a limited degree of SERS enhancement, the introduction of plasmonic gold nanoparticles (AuNPs) greatly improves the SERS signals without sacrificing PSI-MS sensitivity. It is initially revealed that the concentration of AuNPs and the type of analytes highly influence the SERS signals and their variations due to the "coffee ring effect" flow mechanism induced during sampling and the degree of the interfacial interactions (e.g., van der Waals, electrostatic, covalent) between the plasmonic substrate and analyte. Subsequent PSI treatment at high voltage conditions further impacts the overall SERS responses, where the signal sensitivity and homogeneity significantly increase throughout the entire substrate, suggesting the ready migration of adsorbed analytes regardless of their interfacial attractive forces. The PSI-induced notable SERS enhancements are presumably associated with creating unique conditions for local aggregation of the AuNPs to induce effective plasmonic couplings and hot spots (i.e., electromagnetic effect) and for repositioning analytes in close proximity to a plasmonic surface to increase polarizability (i.e., chemical effect). The optimized sampling and PSI conditions are also applicable to multi-analyte analysis by SERS and MS, with greatly enhanced detection capability and signal uniformity.

Keywords: surface enhanced Raman spectroscopy; paper spray ionization (PSI); mass spectrometry; plasmonic nanoparticle; illicit drug analysis; forensics

Citation: Adehinmoye, A.A.; Bondzie, E.H.; Driskell, J.D.; Mulligan, C.C.; Kim, J.-H. Enhanced Sensitivity and Homogeneity of SERS Signals on Plasmonic Substrate When Coupled to Paper Spray Ionization–Mass Spectrometry. *Chemosensors* **2024**, *12*, 175. https://doi.org/10.3390/chemosensors12090175

Received: 11 July 2024
Revised: 18 August 2024
Accepted: 20 August 2024
Published: 2 September 2024

1. Introduction

Developing a method to reliably identify molecular species is highly desirable in forensic science and analytical chemistry [1–4]. Particularly, facilitating an ideal measurement condition, where trace levels of target molecules can be localized and/or properly positioned to generate strong analytical signals, can greatly improve the overall detection sensitivity while minimizing false positives and ambiguous results. In addition, operator safety can be enhanced by significantly reducing the amount of sample necessary for analysis if testing methods require the handling of hazardous chemicals and toxic illicit drugs. Building upon traditional analytical methods (e.g., vibrational spectroscopy-IR and Raman, mass spectrometry-MS, and chromatography-GC and LC) [5–8], the identification of analytes using combined analytical systems can result in a more accurate determination and broader applicability than testing that employs a singular detection technique [1,9]. Although these analytical systems can be designed to demonstrate meaningful test results, the capability of concentrating and isolating pertinent target molecules on the sampling substrate itself can greatly improve the overall sensitivity and selectivity at trace levels. In this sense, a strategy to fabricate a practical single substrate and establish effective sampling

conditions for dual analytical instruments plays a major role in developing reliable and sensitive detection systems.

A mass spectrometer (MS) with ambient ionization capability is of particular interest here, due to the simplicity of sample preparation and the possibility of isolating/concentrating analytes for practical forensic applications [9–11]. Among the many ambient ionization techniques that have been reported [10,12–14], paper spray ionization (PSI) has been demonstrated in the coupling of MS analysis with other instrumental methods at ambient conditions for near real-time analysis. For example, nondestructive molecular vibrational spectroscopy, especially Raman spectroscopy, could provide molecular-specific spectra to serve as a confirmation/complementary technique [15,16]. The PSI treatment often involves the utilization of 2D or 3D untreated paper substrates, which can enable the coupling of MS and Raman for various detection applications, including the medical, forensic, and environmental science fields [9,14,17,18]. Upon replacing bare paper sampling substrates with plasmonic papers, surface-enhanced Raman scattering (SERS) spectroscopy can be coupled with PSI-MS for a more sensitive and selective identification of various molecular species.

As many plasmonic materials have been developed to maximize two enhancement factors, where electromagnetic enhancement (EM) dominates over chemical enhancement (CE), for SERS applications [19–21], paper-based plasmonic substrates could be at the forefront due to their simplicity, affordability, and high-throughput capability. Thus, utilizing a unique plasmonic paper substrate with a high uptake capability of target analytes can improve the entire performance of this combined instrumental method and overcome some limitations associated with typical Raman-based analysis and other single-method approaches. Although combined analyses on shared instrumental platforms have shown promising outcomes for sensitive and selective detection [17,18], there is still room for improvement in the sensing capability by fabricating proper sample treatment methods on plasmonic substrates, allowing for the development of rapid and precise analytical processes.

Here, we utilized a highly practical plasmonic paper, prepared by depositing conventional gold nanoparticles (AuNPs) on a filter paper, and attempted to induce an effective plasmonic coupling environment (i.e., the EM effect) for improved SERS measurements without sacrificing MS sensitivity. Creating an effective plasmonic coupling with typical AuNPs can result in the enhanced detection of various analytes even at trace levels (i.e., properly positioning analytes for greater SERS signals) [22]. Specifically, a mixture of plasmonic NPs and analytes was initially loaded onto the AuNP plasmonic paper to induce plasmonic coupling (via vertically sandwiching analytes). Subsequently, the PSI treatment (i.e., inducing the PSI-MS ionization mechanism) is carried out to change their arrangements across the plasmonic paper to induce additional coupling (via laterally sandwiching analytes). The degree of analyte migration and plasmonic coupling can be monitored by MS and SERS spectra, as the PSI process readily transports adsorbed analytes toward the tip of the triangularly shaped substrate under an applied high voltage. The PSI-induced movement of analytes could readily change the orientation and proximity of the pertinent bonds relative to the surface of plasmonic materials for SERS enhancements (via the EM and CE effects). Thus, SERS analysis can then experimentally show the isolated and concentrated analytes from complex mixtures across the plasmonic sampling substrate. As analytes that possess different interfacial interactions with the plasmonic paper could impact the overall SERS sensitivity, understanding the way the sample treatment impacts the degree of signal enhancement can help modernize the front end of the analytical detection process. As such, paper-based plasmonic substrates with the capability to effectively induce plasmonic coupling can potentially meet the demands for highly practical and precise SERS-based sensing. It is important to remember that combining two independent analytical techniques can readily allow for the sequential acquisition of MS and SERS spectra (referred to as PSI-MS-SERS) in a rapid and reproducible manner to avoid the most common bottleneck in the analytical process—lower throughput due to arduous sample handling and solution application [17]. Considering overall simplicity, higher throughput, and method ruggedness,

a strategy that requires minimal sample preparative steps can be a bonus in developing the entire analytical system. Such a combined analytical approach can undoubtedly assist the advancement of essential techniques for the accurate and rapid detection of various molecular species of interest.

2. Materials and Methods

Gold (III) chloride trihydrate ($HAuCl_4.3H_2O$, 99.99% metals basis), trisodium citrate dihydrate (99%), methanol (99.8%), ethanol (95%), and formic acid (99.5%) were acquired from Fisher Scientific (Fair Lawn, NJ, USA). Whatman Grade 1 filter paper (55 mm circle) was used for all plasmonic paper substrates. Cocaine, 2C-B, fentanyl, and hydrocodone standard solutions were purchased from Cerilliant Corp. (Round Rock, TX, USA) as 1 mg dissolved in 1 mL of methanol. JWH-018 (5 mg) was purchased from Cayman Chemical Company (Ann Arbor, MI, USA). All drug samples were Drug Enforcement Agency (DEA)-exempt. 1,2-Di (4-pyridyl)ethylene (DPE, 97%) and 4-nitrobenzenethiol (NBT, 80%) were purchased from Sigma-Aldrich (St. Louis, MO, USA). Pure water was obtained from a Nanopure water system equipped with a 0.2 μm membrane filter (Barnstead/Thermolyne).

2.1. Preparation of Plasmonic Paper Substrates

Gold nanoparticles (AuNPs) were prepared by a modified thermal reduction using gold salt (2.0 mL, 1.0 wt% of $HAuCl_4 \cdot 3H_2O$) with trisodium citrate dihydrate (1.5 mL of 1 wt%). The extinction spectrum, corresponding to surface plasmon resonance (SPR), of the resulting AuNP solution (~0.25 mg/mL) was examined by a UV–Vis spectrophotometer (Agilent 8453, Agilent Technologies, Santa Clara, CA, USA). The colloidal AuNPs (~60 nm in diameter) exhibiting λ_{max} = ~548 nm with an extinction of ~2.4 were pipetted (10 mL) over Whatman Grade 1 filter papers (55 mm circle) in plastic Petri dishes (~60 mm circle). The papers were fully submerged for 24 h at ambient conditions, while the lids of the Petri dishes were loosely covered to prevent dust contamination. The colored papers were then removed, briefly rinsed with EtOH, and placed in an oven (~50 °C) to dry. The amount of loaded AuNPs onto the papers was roughly estimated by measuring the changes in the SPR peak of colloidal AuNPs (i.e., simply comparing the extinction peak intensity of the AuNP solution before and after the paper treatment) using the standard solution of AuNPs via the Beer–Lambert law [21,23].

2.2. Sampling of Various Analytes onto Plasmonic Paper Substrates

The prepared AuNP-plasmonic papers were cut into the shape of a house-like isosceles triangle to fit into a 3D-printed PSI analysis cartridge, allowing for PSI-MS-SERS analysis on a single paper substrate; this cartridge has been described in previous work [10]. An aliquot of standard solution (1.0 μL) containing an exact concentration of target illicit drug(s) (i.e., fentanyl, 2C-B, hydrocodone, cocaine, and JWH-018) was pipetted on the plasmonic paper and allowed to briefly dry at room temperature. To generate a greater number of hot spots across the plasmonic paper substrate for SERS signal enhancements, several approaches were initially tested, such as using a mixture of illicit drugs with varying concentrations of AuNPs (e.g., extinction of 2.4, 4.8, 7.2, 9.6 and 12) and applying an additional layer of AuNPs (i.e., extinction of 4.8) on the plasmonic surface being treated with a mixture of illicit drugs and AuNPs. Although the initial SERS signals were slightly higher upon utilizing the latter approach, this treatment step required at least 15 min per sample. Considering high throughput and rapid analysis, the former approach, unless noted, was mainly employed in this study. For example, the AuNP solution with the extinction of 2.4 was equally mixed with illicit drugs (i.e., 1:1 *v/v* ratio of AuNP to a drug) to prepare an AuNP-drug mixture exhibiting the extinction of 1.2. An aliquot of this mixture (1.0 μL) was pipetted onto the plasmonic paper for SERS measurements. The same process was taken to prepare a series of mixed solutions containing the analyte and the concentrated AuNPs with the extinction of 4.8, 7.2, 9.6, and 12. In comparison, anisotropic AuNPs with the extinction of 2.4 were mixed with the illicit drugs in a (1:1 *v/v*

ratio) mixture for SERS measurements. Similarly, other analytes, such as DPE and NBT, were also pipetted onto the plasmonic papers for PSI-SERS and individual PSI-MS analyses. To estimate the degree of SERS signal improvement compared to normal Raman under given measurement conditions, the following equation was employed to calculate the analytical SERS enhancement factors (EFs), $EF = (I_{SERS} \times C_{Raman})/(I_{Raman} \times C_{SERS})$ [24,25]. The intensity of Raman (I_{Raman}) was obtained using an aliquot of concentrated analyte solution on a bare filter paper, and the intensity of SERS (I_{SERS}) was acquired using an aliquot of a mixed solution containing analyte and AuNPs on a plasmonic paper. Example calculations are available in the Supplementary Materials section.

2.3. Sampling of Various Analytes on the Plasmonic Paper Substrates

UV–Vis spectrophotometry was used to examine the extinction of all plasmonic nanoparticles before and after loading onto the filter paper under the following conditions: average scans with a data interval of 1.0 nm, an integration time of 0.5 s, and a wavelength range of 190–1100 nm. Pure water was used to blank the instrument before sample analysis. The general size distribution, morphology, and composition of AuNPs on the filter paper were examined by a field emission scanning electron microscope (FESEM, Zeiss Sigma 300 VP equipped with a GEMINI column). All images were collected using a low-voltage source below 2.0 kV. SERS and MS analyses before and after PSI are carried out as follows: Raman spectroscopy was performed with a TSI ProRaman-L system, equipped with a 785 nm laser and a CCD detector cooled to −60 °C. An objective lens (NA = 0.5) focused the laser onto the plasmonic substrate (d = ~100 µm) and the laser power was adjusted to ~10 mW. After applying a mixture of analyte and AuNP solution (1.0 µL) to the plasmonic paper, a minimum of three SERS measurements were initially obtained from several locations (i.e., P1, P2, and P3, as seen in Figure 1). Subsequently, the papers were positioned in a 3D-printed cartridge, which was then inserted in a 3D-printed positioning rig built in-house for PSI-MS analysis. Here, electrical conductivity is produced between a lead electrode and a copper-infused polymeric top plate in contact with the triangular paper substrate, and a high voltage of 5 kV potential relative to the MS inlet capillary was applied to induce ionization. An aliquot of spray solvent (6 µL) was then pipetted onto the paper (i.e., a 1:1 ratio of MeOH and H_2O with 0.1 *v/v*% formic acid). Once a stable PSI spray mechanism was achieved and analysis was completed, SERS spectra were collected from the three different locations on each plasmonic substrate. During PSI-MS, spectra of detected analytes were collected using a Thermo Scientific LCQ fleet quadrupole ion trap mass spectrometer with unit resolution. The mass range of the instrument was typically set between 50 and 500 *m/z* given the relatively small molecular weight of analytes. An averaged MS base scan (n = 3) was collected, followed by tandem MS scans as needed for analyte identification. Similar investigations have also been demonstrated on field-portable MS systems [26].

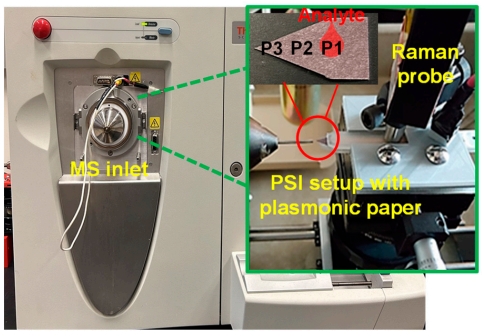

Figure 1. Digital photo of Thermo Scientific LCQ Fleet ion trap MS, with PSI set up for samples on the tip of a 3D-printed cartridge (Note: a 3D-printed positioning rig was used to aid the precise positioning of samples during PSI-MS analysis).

3. Results and Discussion

3.1. Design and Characterization of PSI-SERS Using Plasmonic Paper Substrates with Mixed Solution of AuNPs and Analytes

Figure 2 shows the overall preparation process of plasmonic paper substrates and the subsequent sampling process for PSI-MS and SERS measurements. Initially, gold nanoparticles (AuNPs) were uniformly loaded onto a piece of filter paper, which was cut and mounted on the substrate holder before being placed in the PSI-MS and SERS sample stage. A mixture of drug analytes and AuNPs was then pipetted onto plasmonic paper to induce local aggregation by sandwiching target analytes between plasmonic AuNPs. The paper-based plasmonic substrate can effectively uptake a wide range of analytes to serve as a single sampling substrate for these two instruments, resulting in more sensitive and selective detection. Although plasmonic paper prepared with structurally and compositionally diverse plasmonic NPs (e.g., rods, cubes, etc.) could offer better SERS sensitivity [27–30], these plasmonic NPs are mostly synthesized and stabilized with long-chain capping agents (e.g., CTAB-cetyltrimethylammonium bromide and CTAC-cetyltrimethylammonium chloride), which are observed at high intensity in collected mass spectra (Figure S1). In addition, the preparation of these NPs typically requires multiple steps and is somewhat complicated, which readily limits their practical use. Thus, we focused on utilizing spherical AuNPs prepared by the traditional thermal reduction method in this study and attempted to change their arrangements to amplify SERS sensitivity by strategically utilizing PSI while maintaining overall MS performance. It is also noted that using the spherical AuNPs did not produce any additional background noise under PSI conditions, allowing for yielding simple mass spectra.

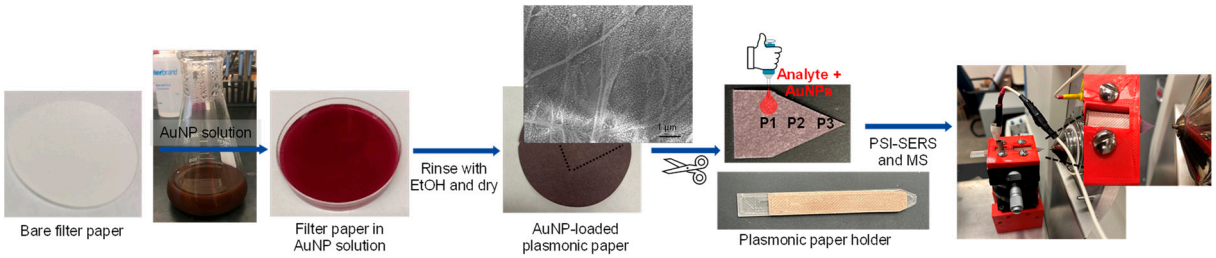

Figure 2. Overall preparation process of plasmonic substrate and sampling method for PSI-MS and SERS measurements.

3.2. Optimization of AuNP Concentration to Induce Optimal SERS Enhancement without Sacrificing MS Performance

Based on previous work [23,31,32], the plasmonic papers prepared with AuNPs possessing an extinction of 2.4 were determined to be ideal for inducing effective plasmonic coupling to maximize SERS enhancement. Thus, the prepared AuNP-loaded plasmonic paper was tested as a single sampling substrate for SERS and PSI-MS, to serve as the initial reference point. To further promote the SERS effect, all analytes were mixed with additional AuNPs before depositing them on the plasmonic paper. As we speculated that the degree of local aggregation and close proximity of analytes to plasmonic materials could be strongly dependent on the concentration of plasmonic NPs, a series of AuNP solutions possessing the extinction of 2.4, 4.8, 7.2, 9.6, and 12, obtained by centrifugation, were mixed with the illicit drug analytes (1:1 *v/v* ratio). It is noted that the extinction band (i.e., SPR) of the concentrated solutions after an equal dilution was mostly comparable, except for the AuNPs with an extinction of 12 (Figure 3A). This slightly lower intensity suggested the inevitable loss of AuNPs or the presence of partial aggregation during the centrifugation and concentration of the solution.

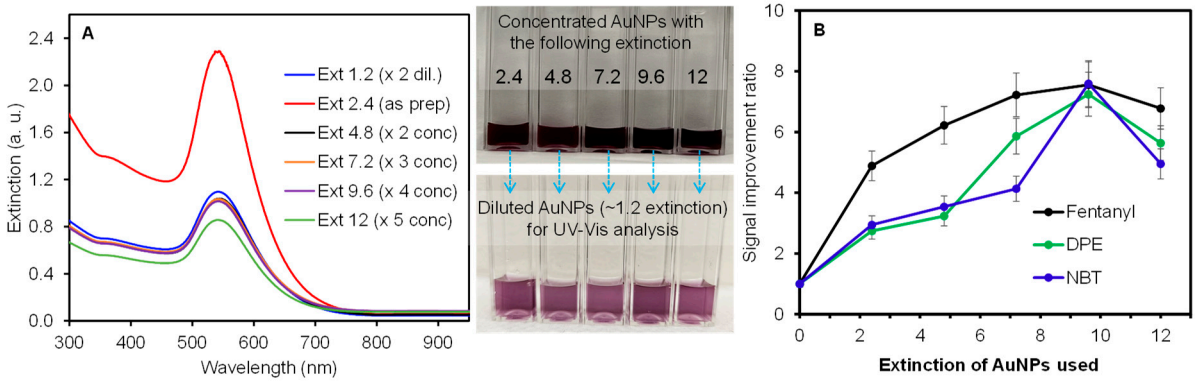

Figure 3. Extinction bands of a series of diluted AuNP solutions and representative photos of concentrated and diluted AuNP solution (**A**) and the SERS signal improvement ratio of three different analytes mixed with AuNPs as a function of concentration (**B**) (error bars from three measurements of each sample using three plasmonic substrates).

It is expected that the introduction of plasmonic AuNPs into the analyte solution enables the initiation of their interfacial interactions [33–35]. In addition, the subsequent application of this mixture onto the plasmonic paper can create an increased probability of producing better SERS environments, considering the well-known two enhancement factors: the EM effect (i.e., increasing plasmonic couplings and hot spots) and the CE effect (i.e., increasing polarizability by positioning analytes close to plasmonic surfaces) [1,19,20,36]. Initially, several analyte solutions without AuNPs were applied to the plasmonic paper (Figure 3B) to serve as baseline SERS signals. These analytes were physically and/or chemically adsorbed onto the preloaded AuNPs (i.e., immobilized) across the substrate, which could prevent the plasmonic NPs from inducing effective local aggregations for ideal EM and/or CE environments. Thus, this type of sampling process could limit the overall degree of SERS enhancements (i.e., difficult to maximize the EM effect). The new sampling conditions involve the co-delivery of additional AuNPs with the analyte solution to allow for the formation of sandwich-type layers with pre-loaded AuNPs in the plasmonic paper. The resulting arrangements can easily induce both lateral and vertical plasmonic couplings and create locally aggregated hot spots to fully benefit the EM and CE effects [19,21,32,37]. The SERS response was then examined using a series of mixed analyte and AuNP solutions containing various concentrations of AuNPs. The signal improvement ratio (benchmarked to the SERS signals obtained by only applying analytes to the plasmonic paper) demonstrates that the co-addition of AuNPs with the analyte solution greatly enhanced the overall SERS performance (e.g., a minimum of 2.7 times) regardless of the type of analyte. As the concentration of co-added plasmonic AuNPs gradually increased, the signal improvement ratios also increased for all analytes. The noticeable improvement clearly indicated the introduction of additional plasmonic couplings and hot spots. The slightly different improvement pattern might be associated with the degree of interactions between analyte and AuNPs (i.e., fentanyl possesses weaker attractive forces, whereas DPE and NBT have stronger electrostatic and covalent interactions, respectively). Interestingly, the use of AuNPs with an extinction of 9.6 resulted in the highest SERS enhancement for all analytes tested. However, further increasing the concentration of AuNPs (i.e., the use of AuNPs with an extinction of 12) in the analyte solutions resulted in an overall reduction in the SERS signals. This observation could possibly be associated with surpassing the optimum point, where the severe aggregations of plasmonic NPs readily decrease the overall areas of the SPR couplings and hot spots, which has also been explained by other research groups [37–39]. In a separate, comparative study, a bare filter paper was also employed to examine the sensitivity of the analyte and a mixture of analyte and AuNP solution (Figure S2). It was evident that the absence of immobilized AuNPs on the filter paper resulted in the negligible detection of the analytes, whereas the AuNP-containing

mixture solutions, particularly for DPE and NBT, possessing stronger interactive forces with AuNPs, clearly displayed measurable SERS signals. The large variations in SERS signals are attributed to the random distribution of locally aggregated analyte-AuNPs on the bare filter paper (i.e., coffee ring effect) [40,41].

3.3. The Influence of PSI-MS Pretreatment on SERS Spectra of Illicit Drugs across the Plasmonic Substrates

After finding the optimum concentration of AuNPs, paper spray ionization (PSI) was carried out to induce the migration of analytes and AuNPs across the plasmonic substrate. The PSI treatment promptly facilitated the movement of the analytes for reliable MS signals, which also significantly influenced the overall SERS responses; MS signal responses are a proxy of analyte movement, as an ionized analyte is only observed in MS spectra after successfully migrating to the tip of the paper substrate and undergoing an electrospray-like mechanism [26]. Based on typical analyte sampling without AuNPs on the plasmonic paper, PSI-induced migration still resulted in notable SERS enhancements, presumably caused by the repositioning of the analytes on the preloaded AuNPs to experience plasmonic coupling environments. Similarly, the distinctive SERS signals were further increased for the co-mixture of analyte molecules and AuNPs after PSI pretreatment. The effective migration of the analytes was confirmed by the homogeneity of SERS spectra across the plasmonic paper substrate, regardless of the sampling methods; more details regarding this phenomenon will be discussed later. It was interesting to observe the influence of the spray solvent on the SERS signals. Specifically, applying pure spray solvent to the plasmonic paper detectably amplified the SERS intensities if the analytes were loaded before or after the solvent treatment. We speculated that this coincidence could be due to the minor contraction of the plasmonic paper upon applying the organic spray solvent, while pure water treatment did not cause any detectable changes in SERS signals. Including this solvent-induced phenomenon, the overall SERS signals distinctively increased at least ~2–3 times, even though some of the analytes were desorbed from the substrate during the PSI pretreatment. To confirm the migration and desorption of the analyte molecules from the substrate, the MS intensities were monitored as a function of time. As the mass spectra display a relative abundance of ionized analytes (e.g., $[M+H]^+$), the intensity of the analyte peak under investigation remained almost unchanged for the PSI duration, from a minimum of 1.9 min to a maximum of 5.2 min depending on the analyte (Table S1). This PSI-induced desorption test indicated that a detectable amount of the drug analytes still remained across the plasmonic paper substrate. Thus, the SERS measurements of the drug analytes were performed after 1 min of PSI treatment in this study.

The SERS intensity of the analytes upon PSI pretreatment could be governed by the distinctively different interfacial interactions between the analytes and the surface of the plasmonic paper. Thus, the PSI-induced migration under ambient conditions was monitored by examining differing locations on the plasmonic paper substrate to understand the way the diverse analytes (and/or plasmonic NPs) migrated across the substrate. Upon applying a droplet of analyte or a mixture of analyte and AuNPs, SERS intensities were initially compared at the sample loading location (P1). It was evident that the utilization of AuNPs effectively enhanced the SERS response (i.e., a higher probability of vertical coupling). It appears that other locations (P2 and P3) still showed detectable SERS signals, probably due to the diffusion of the analytes on the substrate. The subsequent PSI treatment resulted in much more uniform and intense SERS signals across the entirety of plasmonic paper, regardless of the usage of AuNPs, suggesting the migration and repositioning of the analytes to experience the enhanced SERS effect. For example, SERS spectra of 50 ng of pure fentanyl were collected before and after PSI (Figure 4). As is evident, a small peak at 1000 cm^{-1} corresponded to the characteristic fentanyl molecules, which was significantly increased (~3 times) after the PSI treatment. As the PSI process induced the considerable migration of analytes toward the tip of the sample substrate, the P2 and P3 locations showed a notably higher SERS signal. Interestingly, the P1 spot still displayed

increased SERS intensity, but the increase in signal was much lower than the P3 spot under the experimental spray conditions. SERS spectra of a sample mixture containing fentanyl (50 ng) and AuNPs (9.6 extinction) obtained at the P1 location were at least five times greater than those of pure fentanyl, presumably due to the additional formation of local aggregations for plasmonic couplings and hot spots (i.e., the EM effect). After PSI treatment, the entire substrate surface exhibited improved SERS intensities, where P2 and P3 were slightly higher than P1. Even after the migration of fentanyl from P1 to P3, the SERS intensity at P1 was still higher than that prior to PSI-MS. Generally, the SERS signal enhancements for the fentanyl solution containing AuNPs were clearly evident for all locations. It is noted that the intensity of SERS signals uniformly increased across the substrate, even with some loss of the overall amount of analyte by the PSI treatment. Upon testing other illicit drugs (Figure S3), similar SERS results were consistently observed before (significant variations from P1 to P3) and after PSI-MS (high intensity and homogeneity of the signals across the substrate). During the entire PSI period, the corresponding MS signals remained almost unchanged (Figure S4). Separately, several other sample treatment methods associated with applying an additional layer of concentrated AuNPs and utilizing structurally different AuNPs were tested to examine the SERS sensitivity (Figure S5). In some methods, inducing additional plasmonic coupling of AuNPs slightly improved the SERS signals, but seemed to result in loss of effective surface areas due to further aggregations. Other methods required sample processing times that were a bit longer or caused problematic issues for MS analysis (e.g., the appearance of additional MS peaks from shape-guiding surfactant/capping agents, shown in Figure S1). Considering the simplicity and practicability, applying a mixture of analyte and AuNPs appeared to be ideal for the remaining experiments.

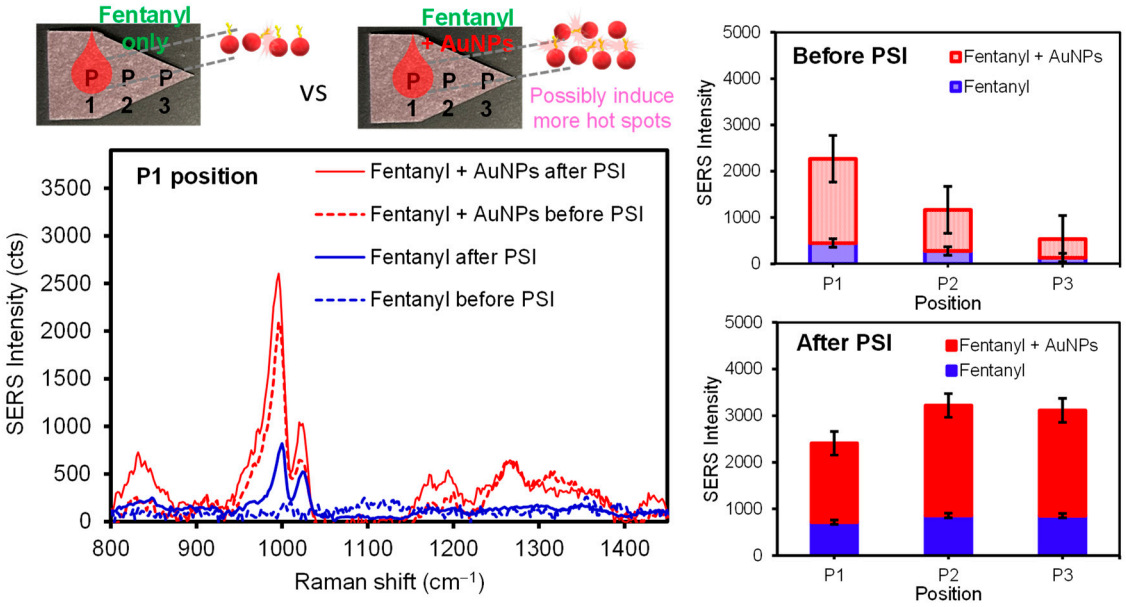

Figure 4. Representative SERS spectra of fentanyl and a mixture of fentanyl and AuNPs and their average signal intensities at several paper positions before and after PSI.

3.4. The Influence of PSI-MS Pretreatment on SERS Spectra of Other Organic Molecules with Strong Interface Interactions across the Plasmonic Substrates

As the above illicit drug molecules possess relatively weak interactions (e.g., van der Waals and hydrogen bonding) with the plasmonic substrate, analytes with stronger interactive forces could impact their overall diffusion and migration before and after PSI. This speculation led us to investigate additional target analytes possessing electrostatic and covalent interactions with plasmonic substrates and NPs. For example, the SERS spectra of 1,2-di(4-pyridyl)ethylene (DPE) that induces electrostatic interactions with the plasmonic paper were examined before and after PSI (Table 1 and Figure S6). Without

mixing additional AuNPs with the sample solution, several peaks of DPE (50 ng) appeared at 1020 cm^{-1}, 1200 cm^{-1}, 1340 cm^{-1}, 1610 cm^{-1}, and 1636 cm^{-1}. For simple comparison, the intensity of the main peak at 1610 cm^{-1} was carefully monitored as a function of the PSI pretreatment. The SERS peak appeared to be very intense at the P1 spot where the DPE solution was applied, significantly weakened at P2, and marginally detectable at P3. After PSI, the notable increase in intensities and uniformity of SERS spectra at all three locations directly indicated the effective migration of DPE across the plasmonic paper. Upon co-mixing additional AuNPs with the sample solution, the intensity of DPE increased at least 3 times at the initial spot (P1), suggesting the presence of effective plasmonic couplings (i.e., sandwiching DPE with AuNPs laterally and vertically). The SERS intensity at the P2 spot notably decreased but was still much greater than that of DPE without AuNPs. However, the peak intensity at P3 was much weaker than that of DPE without AuNPs, which could be due to the limited diffusion of DPE-bound AuNPs. After PSI, the DPE peaks were uniformly increased across the entire sample substrate regardless of the sample spots, where the relative increase in SERS signal gradually increased (i.e., P1 < P2 < P3). In contrast to the illegal drugs above, the tip of the plasmonic paper (P3) displayed the lowest, and the original sample spot (P1) maintained the highest SERS signals, which probably implies the somewhat restricted migration of DPE-bound AuNPs. Although one can speculate that DPE could be accumulated near the tip area after PSI to display higher SERS signals, slightly lower SERS intensity could suggest the slightly inefficient migration of the analyte due to the strong electrostatic interactive forces with the plasmonic substrate.

Table 1. SERS intensity of neat DPE and a mixture of DPE and AuNPs before and after PSI at three different spots on the plasmonic substrate (analytical EFs in parenthesis).

	50 ng DPE		50 ng DPE + AuNPs	
Position	Before PSI	After PSI	Before PSI	After PSI
P1 (sampling position)	2497 ± 25 (~1.35×10^5)	4427 ± 40 (~2.39×10^5)	9418 ± 37 (~5.09×10^5)	15,635 ± 41 (~8.45×10^5)
P2 (middle)	598 ± 30	4249 ± 57	2215 ± 32	12,320 ± 36
P3 (tip)	164 ± 54	4004 ± 60	85 ± 34	11,718 ± 33
% RSD	~114	~5	~125	~16

To examine the influence of stronger interfacial interactions (i.e., a covalent bond) between the analyte and plasmonic substrate, 4-nitrobenzenethiol (NBT) was treated under the same conditions (Figure 5 and Table S2). When an aliquot of pure NBT solution was dropped on the plasmonic paper, detectable SERS signals were only observed at the P1 and P2 spots. The near absence of detectable peaks at P3 (S/N < 3) was presumably due to the completely inhibited diffusion of NBT molecules across the plasmonic paper (i.e., the formation of a S-Au covalent bond). This experimental observation suggested that the way the analytes interact with the plasmonic substrate certainly influences the degree of their diffusion. Specifically, the illicit drug molecules possessing weak interfacial interactions with the plasmonic paper diffused far more than DPE and NBT with strong electrostatic and covalent interactions. After the PSI treatment for 1 min, SERS signals were consistently intensified for all three locations, still implying the migration of the NBT analyte. Upon applying the mixed solution of NBT and AuNPs, the initial SERS intensities at P1 and P2 were at least 10-fold and 25-fold higher than those of pure NBT, presumably due to the SERS effect (CE-formation of the covalent bond and EM-formation of a sandwiched geometry). An aliquot of the mixed solution of NBT and AuNPs already contains covalently bound NBT on AuNPs, which can be loaded onto the AuNP plasmonic paper (e.g., effectively undergo the gravity-driven sandwiching process between the NBT-AuNPs in solution and AuNPs on the paper substrate). This sandwiched structure readily enhances plasmonic coupling and hot spots to boost SERS signals that could provide the highly sensitive

detection of Raman active molecules. Again, there were no detectable signals at P3 due to the insufficient diffusion of NBT-AuNPs. After the PSI treatment, SERS signals increased across the entire substrate, where the P2 and P3 spots displayed much greater SERS signals (>25,000 cts). These noticeable changes suggested the migration of loosely adsorbed NBT-AuNPs toward the tip of the substrate, where a droplet of mixture applied to the plasmonic substrate might not instantaneously allow for the firm immobilization of NBT-AuNPs. Similar to DPE, the intensity of the NBT peak at the tip of the substrate (P3) was slightly lower than the original spot (P1) and the middle spot (P2). The highest peak intensity at P1 could also be explained by the slower movement of the NBT analyte due to the strong bond formation with AuNPs. If the PSI treatment solely induced the migration of the NBT molecules (i.e., decreasing the probability of sandwiching NBT between AuNPs), one can speculate that the SERS intensities could be comparable to those of the pure NBT after PSI (~5000 cts).

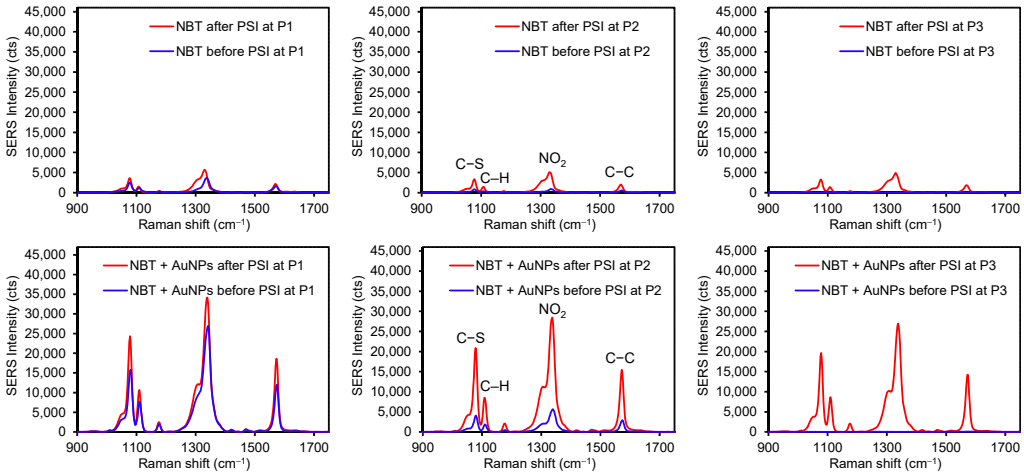

Figure 5. Representative SERS spectra of NBT (top) and a mixture of NBT and AuNPs (bottom) before and after PSI at three different spots on the plasmonic sample substrate (P1 for the original sample spot and P2 for in between P1 and P3, and P3 for the tip of the substrate).

Unlike the preparation of plasmonic paper involving the firm immobilization of AuNPs on the filter paper, the introduction of a fresh droplet containing the analyte mixed with AuNPs could allow for the loose deposition of AuNPs onto the plasmonic paper. After rapidly drying in room air, the subsequent PSI treatment could induce the possible migration of these lightly bound AuNPs on the plasmonic substrate. To confirm the possible migration of AuNPs under PSI conditions, a droplet of the mixed solution was applied to bare filter paper (Figure S7). After the quick drying, the color of the droplets on the paper was examined before and after PSI. The color at the P1 spot appeared to gradually fade away after PSI, implying the probable movement of the AuNPs. SEM images after PSI showed that most AuNPs remained at the initial P1 spot, but a few AuNPs were randomly detectable near the tip of the paper (P3), which confirmed the migration of the applied AuNPs. In contrast, examining the movement of preloaded AuNPs on the plasmonic paper was very challenging given the densely packed AuNPs on the rough paper substrate. It appears that the color of the plasmonic substrate was negligibly changed after applying a droplet of the mixed solution. In addition, the color of the substrate remained the same even after the PSI treatment, presumably because most preloaded AuNPs were strongly immobilized on the paper while only a few AuNPs were migrated. SEM images of the plasmonic paper were not able to resolve any morphological changes after applying the droplet and the PSI treatment. However, the degree of SERS enhancements toward the tip of the plasmonic substrate suggested the possibility of inducing the movement of post-loaded AuNPs with analytes during PSI. Considering the migration degree of the post-loaded AuNPs, the SERS enhancements appeared to be far greater than expected. Thus, a more

in-depth study is needed to better understand the relationships between the PSI-induced migration of AuNPs and the level of SERS enhancements. Regardless of these concerns, it was evident that the introduction of plasmonic AuNPs into the analyte solution greatly improved the SERS-based sensing capability, and the PSI treatment provides homogenous and consistent signals across the sample substrate.

3.5. The Influence of PSI-MS Pretreatment on SERS Spectra for Mixed Analytes

Furthermore, the illicit drugs cocaine and JWH-018 (a synthetic cannabinoid) were mixed with AuNPs to demonstrate the possibility of discriminating between two different analytes before and after the PSI pretreatment (Figures 6 and S8). Several peaks for JWH-018 at 1364 cm^{-1} ($\nu_{C=C}$) and 768 cm^{-1} (ring breathing) were detectably higher than those of the cocaine peak at 1010 cm^{-1} (ν_{C-C} in the aromatic ring) [42,43]. As these drug molecules possess weak interfacial interactions with the surface of AuNPs, the diffusion process promptly allowed for their physical adsorption across the plasmonic paper, which was confirmed by the SERS intensity variations (e.g., P1 to P3) before PSI. The subsequent PSI treatment readily increased the SERS signals for both compounds (at least ~3–4 times at P1 and P2, and ~8 times at P3). The degree of peak enhancements for the mixture was far greater than that for individual drugs, which could be caused by matrix effects and/or the presence of common molecular backbones (i.e., the overlap of vibrational energy levels) [1,44–46]. As observed above, the homogeneity of the signals improved again throughout the substrate after the PSI treatment. Specifically, the initial intensity variations between P1 and P3 were ~3 and ~4 times for cocaine and JWH-018, respectively. After the PSI treatment, the variations in SERS intensity were significantly reduced for cocaine (~1.5 times) and JWH-018 (~1.6 times). Separately, the relative abundance of mass spectra for JWH-018 was higher than cocaine, possibly associated with the ionization efficiency under our PSI-MS conditions. This mixed analyte analysis also suggested the possibility of improving the identification capability of our system by utilizing plasmonic AuNPs and PSI treatment. Along with fabricating a multi-purpose plasmonic paper, developing an effective sample handling method can still improve the overall sensitivity and selectivity of both PSI-MS and SERS analyses.

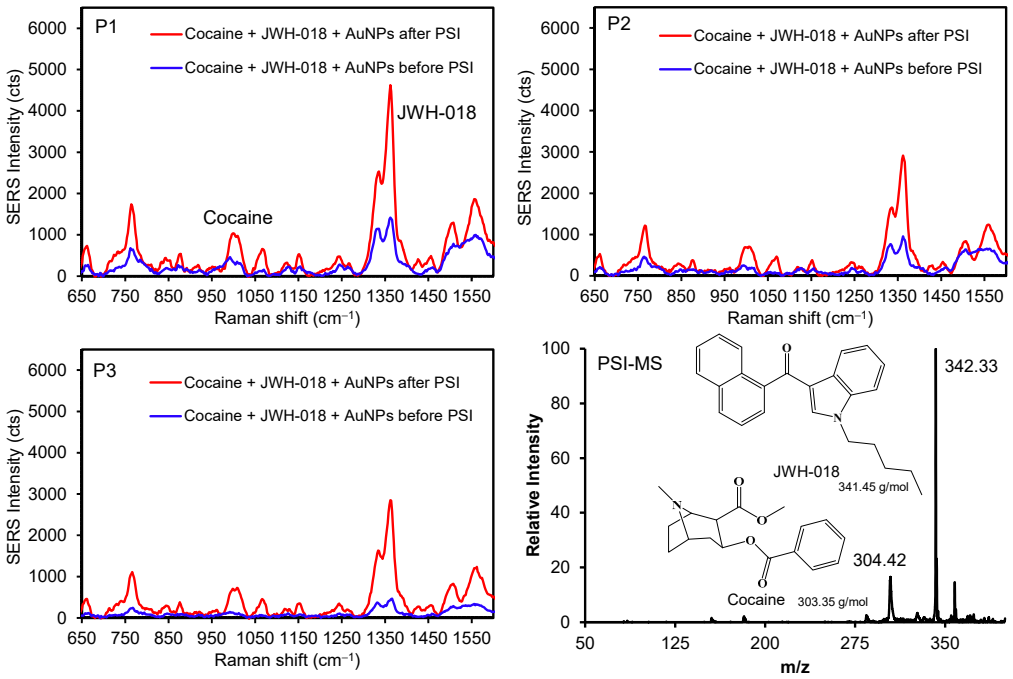

Figure 6. SERS spectra of illicit drug mixtures with and without AuNPs at three different spots before and after PSI (P1 for the initial sample location) and representative PSI-MS.

4. Conclusions

A simple sampling protocol is established using conventional plasmonic AuNPs and filter paper for a dual PSI-MS and SERS system. Applying a mixed solution of AuNPs and target analytes to the plasmonic paper greatly improves the detection capability of SERS without losing PSI-MS sensitivity. The analytes exhibiting relatively weak interfacial interactions are widely spread on the plasmonic substrate, whereas the analytes possessing relatively stronger interfacial interactions display limited diffusion. Upon carrying out the PSI treatment, all SERS signals become highly uniform and notably intense throughout the entire plasmonic paper substrate, regardless of the type of analytes, presumably indicating the effective repositioning of the analytes to experience the SERS effect. As expected, the PSI treatment induced a slightly limited migration of the analytes possessing relatively strong interfacial interactions with the plasmonic paper. The proper utilization of PSI and plasmonic NPs can lead to the reliable identification and confirmation of various analytes, including illicit drug mixtures, by the combined analytical techniques. Developing an inexpensive paper-based sampling substrate and establishing amenable analyte treatment conditions for PSI-MS and SERS can allow for high throughput fabrication to fulfill the demands for modernized sensing systems. Of particular utility is the observation of signal uniformity during SERS analysis, which in turn provides great flexibility in the SERS analysis spot (i.e., the focal point location of the SERS laser source for detection). A further boon to such a method is fieldability, and several reports of the use of portable/handheld devices for coupling both PSI-MS and SERS can be found in the literature [18,47,48]. These advancements, integrated with fewer sample preparative steps, could allow for simplistic use by non-scientist operators, who would be tasked with operating such devices in areas such as forensics, homeland security, and environmental protection [49].

Supplementary Materials: The following supporting information can be downloaded at: https://www.mdpi.com/article/10.3390/chemosensors12090175/s1, Figure S1. An example of a surfactant peak obtained by PSI-MS using a mixture of cetyltrimethylammonium chloride (CTAC)-modified AuNPs and cocaine (note: the *m/z* of the CTAC surfactant was protonated CTAC without Cl ion); Figure S2. Raman intensity of three different analytes on a bare filter paper (error bars from at least three measurements of each sample); Figure S3. SERS response of three representative illicit drug analytes with AuNPs on the plasmonic paper before and after PSI (SERS signal fluctuations across the sample substrate before and after shown in Tables); Figure S4. Typical PSI-MS of tested analytes with total ion chronograms (TICs) inset; Figure S5. SERS response of five illicit drugs under other sample treatments (e.g., applying an additional layer of structurally different AuNPs); Figure S6. SERS spectra of DPE and a mixture of DPE and AuNPs on the plasmonic paper before and after the PSI treatment (from P1 to P3 spots); Figure S7. Digital photos and representative SEM images of a mixture of analyte and AuNPs on bare filter papers and the plasmonic paper before and after the PSI treatment; Figure S8. Example SERS spectra of JWH-018 and cocaine on the plasmonic paper [J presents JWH-018 peaks at ~670 cm^{-1} (deformation of naphthalene ring), ~770 cm^{-1} (ring breading of indole), and ~1360 cm^{-1} (C=C of naphthalene ring), and C presents cocaine peaks at ~880 cm^{-1} (C-C of pyrrolidine ring), ~1010 cm^{-1} (C-C of aromatic ring), and ~1260 cm^{-1} (tropane moiety)]; Table S1. Average desorption time of illicit drugs from the plasmonic paper via PSI (monitored by a mass spectrometer); Table S2. SERS intensity of bare NBT and a mixture of NBT and AuNPs before and after PSI at three different spots on the sample substrate (analytical EFs in parenthesis).

Author Contributions: Conceptualization, J.D.D., C.C.M. and J.-H.K.; methodology, A.A.A. and E.H.B.; validation, A.A.A. and E.H.B.; formal analysis, A.A.A. and E.H.B.; investigation, A.A.A.; writing—original draft preparation, A.A.A. and J.-H.K.; writing—review and editing, J.D.D., C.C.M. and J.-H.K.; supervision, C.C.M. and J.-H.K.; project administration, J.D.D., C.C.M. and J.-H.K.; funding acquisition, J.D.D., C.C.M. and J.-H.K. All authors have read and agreed to the published version of the manuscript.

Funding: The FESEM multi-user facility was acquired with the support from the Division of Material Research (DMR), National Science Foundation (NSF) (Award # 2116612). This project was also supported in part by Award No. 2017-R2-CX-0022, from the National Institute of Justice, Office of Justice Programs, U.S. Department of Justice. The opinions, findings, and conclusions or recommendations

expressed in this publication are those of the authors and do not necessarily reflect those of the Department of Justice.

Institutional Review Board Statement: Not applicable.

Informed Consent Statement: Not applicable.

Data Availability Statement: All data are contained within the article or figure material.

Acknowledgments: We acknowledge the support from the Department of Chemistry of Illinois State University.

Conflicts of Interest: The authors declare no conflicts of interest.

References

1. Moldovan, R.; Vereshchagina, E.; Milenko, K.; Jacob, B.-C.; Bodoki, A.E.; Falamas, A.; Tosa, N.; Muntean, C.M.; Farcau, C.; Bodoki, E. Review on combining surface-enhanced Raman spectroscopy and electrochemistry for analytical applications. *Anal. Chim. Acta* **2022**, *1209*, 339250. [CrossRef]
2. Restaino, S.M.; White, I.M. A critical review of flexible and porous SERS sensors for analytical chemistry at the point-of-sample. *Anal. Chim. Acta* **2018**, *1060*, 17–29. [CrossRef]
3. Teixeira, A.; Hernández-Rodríguez, J.F.; Wu, L.; Oliveira, K.; Kant, K.; Piairo, P.; Diéguez, L.; Abalde-Cela, S. Microfluidics-driven fabrication of a low cost and ultrasensitive SERS-based paper biosensor. *Appl. Sci.* **2019**, *9*, 1387. [CrossRef]
4. Gwon, Y.; Kim, J.-H.; Lee, S.-W. Quantification of plasma dopamine in depressed patients using silver-enriched silicon nanowires as SERS-active substrates. *ACS Sens.* **2024**, *9*, 870–882. [CrossRef]
5. Holtkamp, H.U.; Aguergaray, C.; Prangnell, K.; Pook, C.; Amirapu, S.; Grey, A.; Simpson, C.; Nieuwoudt, M.; Jarrett, P. Raman spectroscopy and mass spectrometry identifies a unique group of epidermal lipids in active discoid lupus erythematosus. *Sci. Rep.* **2023**, *13*, 16452. [CrossRef]
6. Lo, Y.-H.; Hiramatsu, H. Online liquid chromatography–Raman spectroscopy using the vertical flow method. *Anal. Chem.* **2020**, *92*, 14601–14607. [CrossRef]
7. Liangsupree, T.; Multia, E.; Saarinen, J.; Ruiz-Jimenez, J.; Kemell, M.; Riekkola, M.-L. Raman spectroscopy combined with comprehensive gas chromatography for label-free characterization of plasma-derived extracellular vesicle subpopulations. *Anal. Biochem.* **2022**, *647*, 114672. [CrossRef]
8. Klingler, S.; Hniopek, J.; Stach, R.; Schmitt, M.; Popp, J.; Mizaikoff, B. Simultaneous infrared spectroscopy, Raman spectroscopy, and luminescence sensing: A multispectroscopic analytical platform. *ACS Meas. Sci. Au* **2022**, *2*, 157–166. [CrossRef]
9. Fedick, P.W.; Morato, N.M.; Pu, F.; Cooks, R.G. Raman spectroscopy coupled with ambient ionization mass spectrometry: A forensic laboratory investigation into rapid and simple dual instrumental analysis techniques. *Int. J. Mass Spectrom.* **2020**, *452*, 116326. [CrossRef]
10. Rankin-Turner, S.; Sears, P.; Heaney, L.M. Applications of ambient ionization mass spectrometry in 2022: An annual review. *Anal. Sci. Adv.* **2023**, *4*, 133–153. [CrossRef]
11. Brown, H.M.; McDaniel, T.J.; Doppalapudi, K.R.; Mulligan, C.C.; Fedick, P.W. Rapid, in situ detection of chemical warfare agent simulants and hydrolysis products in bulk soils by low-cost 3D-printed cone spray ionization mass spectrometry. *Analyst* **2021**, *146*, 3127–3136. [CrossRef]
12. Feider, C.L.; Krieger, A.; DeHoog, R.J.; Eberlin, L.S. Ambient ionization mass spectrometry: Recent developments and applications. *Anal. Chem.* **2019**, *91*, 4266–4290. [CrossRef]
13. Shi, L.; Habib, A.; Bi, L.; Hong, H.; Begum, R.; Wen, L. Ambient ionization mass spectrometry: Application and prospective. *Crit. Rev. Anal. Chem.* **2022**, 1–50. [CrossRef]
14. McBride, E.M.; Mach, P.M.; Dhummakupt, E.S.; Dowling, S.; Carmany, D.O.; Demond, P.S.; Rizzo, G.; Manicke, N.E.; Glaros, T. Paper spray ionization: Applications and perspectives. *TrAC Trends Anal. Chem.* **2019**, *118*, 722–730. [CrossRef]
15. Hashimoto, K.; Badarla, V.R.; Kawai, A.; Ideguchi, T. Complementary vibrational spectroscopy. *Nat. Commun.* **2019**, *10*, 4411. [CrossRef]
16. Oksenberg, E.; Shlesinger, I.; Tek, G.; Koenderink, A.F.; Garnett, E.C. Complementary surface-enhanced Raman scattering (SERS) and IR absorption spectroscopy (SEIRAS) with nanorods-on-a-mirror. *Adv. Funct. Mater.* **2023**, *33*, 2211154. [CrossRef]
17. Fedick, P.W.; Bills, B.J.; Manicke, N.E.; Cooks, R.G. Forensic sampling and analysis from a single substrate: Surface-enhanced Raman spectroscopy followed by paper spray mass spectrometry. *Anal. Chem.* **2017**, *89*, 10973–10979. [CrossRef]
18. Burr, D.S.; Fatigante, W.L.; Lartey, J.A.; Jang, W.; Stelmack, A.R.; McClurg, N.W.; Standard, J.M.; Wieland, J.R.; Kim, J.-H.; Mulligan, C.C.; et al. Integrating SERS and PSI-MS with dual purpose plasmonic paper substrates for on-site illicit drug confirmation. *Anal. Chem.* **2020**, *92*, 6676–6683. [CrossRef]
19. Ding, S.-Y.; You, E.-M.; Tian, Z.-Q.; Moskovits, M. Electromagnetic theories of surface-enhanced Raman spectroscopy. *Chem. Soc. Rev.* **2017**, *46*, 4042–4076. [CrossRef]
20. Sharma, B.; Cardinal, M.F.; Kleinman, S.L.; Greeneltch, N.G.; Frontiera, R.R.; Blaber, M.G.; Schatz, G.C.; Van Duyne, R.P. High-performance SERS substrates: Advances and challenges. *MRS Bull.* **2013**, *38*, 615–624. [CrossRef]

21. Lartey, J.A.; Harms, J.P.; Frimpong, R.; Mulligan, C.C.; Driskell, J.D.; Kim, J.-H. Sandwiching analytes with structurally diverse plasmonic nanoparticles on paper substrates for surface enhanced Raman spectroscopy. *RSC Adv.* **2019**, *9*, 32535–32543. [CrossRef]
22. Qi, Z.; Akhmetzhanov, T.; Pavlova, A.; Smirnov, E. Reusable SERS substrates based on gold nanoparticles for peptide detection. *Sensors* **2023**, *23*, 6352. [CrossRef]
23. Kim, J.-H.; Twaddle, K.M.; Cermak, L.M.; Jang, W.; Yun, J.; Byun, H. Photothermal heating property of gold nanoparticle loaded substrates and their SERS response. *Colloids Surf. A* **2016**, *498*, 20–29. [CrossRef]
24. Rodrigues, D.C.; de Souza, M.L.; Souza, K.S.; dos Santos, D.P.; Andrade, G.F.S.; Temperini, M.L.A. Critical assessment of enhancement factor measurements in surface-enhanced Raman scattering on different substrates. *Phys. Chem. Chem. Phys.* **2015**, *17*, 21294–21301. [CrossRef]
25. Le Ru, E.C.; Blackie, E.; Meyer, M.; Etchegoin, P.G. Surface enhanced Raman scattering enhancement factors: A comprehensive study. *J. Phys. Chem. C* **2007**, *111*, 13794–13803. [CrossRef]
26. Lawton, Z.E.; Traub, A.; Fatigante, W.L.; Mancias, J.; O'Leary, A.E.; Hall, S.E.; Wieland, J.R.; Oberacher, H.; Gizzi, M.C.; Mulligan, C.C. Analytical validation of a portable mass spectrometer featuring interchangeable, ambient ionization sources for high throughput forensic evidence screening. *J. Am. Soc. Mass Spectr.* **2017**, *28*, 1048–1059. [CrossRef]
27. Ashley, M.J.; Bourgeois, M.R.; Murthy, R.R.; Laramy, C.R.; Ross, M.B.; Naik, R.R.; Schatz, G.C.; Mirkin, C.A. Shape and size control of substrate-grown gold nanoparticles for surface-enhanced Raman spectroscopy detection of chemical analytes. *J. Phys. Chem. C* **2018**, *122*, 2307–2314. [CrossRef]
28. Tian, F.; Bonnier, F.; Casey, A.; Shanahan, A.E.; Byrne, H.J. Surface enhanced Raman scattering with gold nanoparticles: Effect of particle shape. *Anal. Methods* **2014**, *6*, 9116–9123. [CrossRef]
29. Nikoobakht, B.; El-Sayed, M.A. Surface-enhanced Raman scattering on aggregated gold nanorods. *J. Phys. Chem. A* **2003**, *107*, 3372–3378. [CrossRef]
30. Rycenga, M.; Langille, M.R.; Personick, M.L.; Ozel, T.; Mirkin, C.A. Chemically isolating hot spots on concave nanocubes. *Nano Lett.* **2012**, *12*, 6218–6222. [CrossRef]
31. Ngo, Y.H.; Li, D.; Simon, G.P.; Garnier, G. Effect of cationic polyacrylamides on the aggregation and SERS performance of gold nanoparticles-treated paper. *J. Colloid Interface Sci.* **2013**, *392*, 237–246. [CrossRef] [PubMed]
32. Jang, W.; Byun, H.; Kim, J.-H. Rapid preparation of paper-based plasmonic platforms for SERS applications. *Mater. Chem. Phys.* **2020**, *240*, 122124. [CrossRef]
33. Fusaro, M.; Leś, A.; Stolarczyk, E.U.; Stolarczyk, K. Computational modeling of gold nanoparticle interacting with molecules of pharmaceutical interest in water. *Molecules* **2023**, *28*, 7167. [CrossRef]
34. Osinkina, L. *Interactions of Molecules in the Vicinity of Gold Nanoparticles*; LMU: Munich, Germany, 2014.
35. Rafiee, M.; Chandra, S.; Ahmed, H.; McCormack, S.J. Optimized 3D finite-difference-time-domain algorithm to model the plasmonic properties of metal nanoparticles with near-unity accuracy. *Chemosensors* **2021**, *9*, 114. [CrossRef]
36. Haynes, C.L.; Van Duyne, R.P. Plasmon-sampled surface-enhanced Raman excitation spectroscopy. *J. Phys. Chem. B* **2003**, *107*, 4726–4733. [CrossRef]
37. Zhu, Z.; Zhu, T.; Liu, Z. Raman scattering enhancement contributed from individual gold nanoparticles and interparticle coupling. *Nanotechnology* **2004**, *15*, 357–364. [CrossRef]
38. Lee, M.; Oh, K.; Choi, H.-K.; Lee, S.G.; Youn, H.J.; Lee, H.L.; Jeong, D.H. Subnanomolar sensitivity of filter paper-based SERS sensor for pesticide detection by hydrophobicity change of paper surface. *ACS Sens.* **2018**, *3*, 151–159. [CrossRef]
39. Kho, K.W.; Shen, Z.X.; Zeng, H.C.; Soo, K.C.; Olivo, M. Deposition method for preparing SERS-active gold nanoparticle substrates. *Anal. Chem.* **2005**, *77*, 7462–7471. [CrossRef]
40. Yan, X.; Zhu, W.; Wang, Y.; Wang, Y.; Kong, D.; Li, M. "Coffee Ring" fabrication and its application in Aflatoxin detection based on SERS. *Chemosensors* **2023**, *11*, 22. [CrossRef]
41. Rourke-Funderburg, A.S.; Walter, A.B.; Carroll, B.; Mahadevan-Jansen, A.; Locke, A.K. Development of a low-cost paper-based platform for coffee ring-assisted SERS. *ACS Omega* **2023**, *8*, 33745–33754. [CrossRef]
42. Deriu, C.; Conticello, I.; Mebel, A.M.; McCord, B. Micro solid phase extraction surface-enhanced Raman spectroscopy (μ-SPE/SERS) screening test for the detection of the synthetic cannabinoid JWH-018 in oral fluid. *Anal. Chem.* **2019**, *91*, 4780–4789. [CrossRef]
43. de Oliveira Penido, C.A.F.; Pacheco, M.T.T.; Lednev, I.K.; Silveira, L., Jr. Raman spectroscopy in forensic analysis: Identification of cocaine and other illegal drugs of abuse. *Raman Spectrosc.* **2016**, *47*, 28–38. [CrossRef]
44. Soper, S.A.; Kuwana, T. Matrix-isolated surface-enhanced Raman spectroscopy (SERS): The role of the supporting matrix. *Appl. Spectrosc.* **1989**, *43*, 1180–1197. [CrossRef]
45. Yang, C.W.; Zhang, X.; Yuan, L.; Wang, Y.K.; Sheng, G.P. Deciphering the microheterogeneous repartition effect of environmental matrix on surface-enhanced Raman spectroscopy (SERS) analysis for pollutants in natural waters. *Water Res.* **2023**, *232*, 119668. [CrossRef] [PubMed]
46. Lu, G.; Johns, A.J.; Neupane, B.; Phan, H.T.; Cwiertny, D.M.; Forbes, T.Z.; Haes, A.J. Matrix-independent surface-enhanced Raman scattering detection of uranyl using electrospun amidoximated polyacrylonitrile mats and gold nanostars. *Anal. Chem.* **2018**, *90*, 6766–6772. [CrossRef] [PubMed]
47. Erkok, S.D.; Gallois, R.; Leegwater, L.; Gonzalez, P.C.; van Asten, A.; McCord, B. Combining surface-enhanced Raman spectroscopy (SERS) and paper spray mass spectrometry (PS-MS) for illicit drug detection. *Talanta* **2024**, *278*, 126414. [CrossRef]

48. Fedick, P.W.; Morato, N.; Cooks, R.G. Identification and confirmation of fentanyl on paper using portable surface enhanced Raman spectroscopy and paper spray Ionization mass spectrometry. *J. Am. Mass Spectrom.* **2020**, *31*, 735–741. [CrossRef]
49. Evans-Nguyen, K.; Stelmack, A.R.; Clowser, P.C.; Holtz, J.M.; Mulligan, C.C. Fieldable mass spectrometry for forensic science, homeland security, and defense applications. *Mass Spectrom. Rev.* **2021**, *40*, 628–646. [CrossRef]